

# Synthesis and Properties of Carbazole Main Chain Copolymers with Oxadiazole Pendant toward Bipolar Polymer Host: Tuning the HOMO/LUMO Level and Triplet Energy

Kai Zhang,<sup>†</sup> Youtian Tao,<sup>†</sup> Chuluo Yang,<sup>\*,†</sup> Han You,<sup>‡</sup> Yang Zou,<sup>†</sup> Jingui Qin,<sup>†</sup> and Dongge Ma<sup>\*,‡</sup>

Department of Chemistry, Hubei Key Laboratory on Organic and Polymeric Optoelectronic Materials, Wuhan University, Wuhan 430072, P. R. China, and State Key Laboratory of Polymer Physics and Chemistry, Changchun Institute of Applied Chemistry, Chinese Academy of Sciences, Changchun 130022, People's Republic of China

Received August 18, 2008

Three new carbazole copolymers, poly(9-(2,5-diarene-[1,3,4]oxadiazole)-carbazole-*alt*-9-(2-ethylhexyl)-carbazole-3,6-diyl)s (**P1**), poly(9-(2,5-diarene-[1,3,4]oxadiazole)-2,7-carbazole-*alt*-9-(2-ethylhexyl)-3,6-carbazole-diyl)s (**P2**), and poly(9-(2,5-diarene-[1,3,4]oxadiazole)-carbazole-*alt*-9-(2-ethylhexyl)-carbazole-2,7-diyl)s (**P3**), were synthesized by the Suzuki coupling reaction. The copolymers were characterized by <sup>1</sup>H NMR, <sup>13</sup>C NMR, and elements analysis, and their molecular weights were estimated using gel permeation chromatography. The TGA and DSC results revealed their good thermal stability with high glass-transition temperatures ( $T_g$ ) at 211 °C (**P1**), 194 °C (**P2**), and 208 °C (**P3**), respectively. The copolymers exhibited blue emission with significantly improved fluorescence quantum efficiencies compared to their analogous polymers. The triplet energies of **P1**, **P2**, and **P3** were determined to be 2.52, 2.42, and 2.32 eV, respectively, from their phosphorescent spectra at 77 K. The HOMO/LUMO levels of the carbazole copolymers can be tuned by different coupling positions and substitution at the 9-position of carbazole. **P1** by connecting carbazole units via their 3 (6) positions shifts the HOMO/LUMO levels to higher energy compared to **P2** via 2 (7) positions, whereas replacing alkyl groups at the 9-position of carbazole with electron-withdrawing diaryl-1,3,4-oxadiazole group shifts the HOMO/LUMO levels to lower energy. Finally, polymer light-emitting diodes employing the **P1–3** as host and bis(2,4-diphenylquinolinato-*N,C*<sup>2</sup>)iridium(acetylacetonate) (Ir(ppq)<sub>2</sub>(acac)) as guest were constructed and characterized electrically.

## Introduction

Phosphorescent polymer light-emitting diodes (PLEDs) with heavy metal complexes doped in polymer host have attracted considerable attention for their convenient preparation from solution by spin-coating or inkjet printing method and 100% internal quantum efficiency in theory by fully utilizing both singlet and triplet excitons.<sup>1</sup> It is desirable that the polymer host has large enough bandgap for effective energy transfer to guest, and good carrier transport properties for a balanced carriers recombination in emitting layer, as well as energy-level matching with electrodes for effective charge injection.<sup>2</sup> However, most polymer hosts prefer to transport holes than electrons. To improve the transportation of electrons in PLEDs, researchers usually blends *p*-type polymer hosts with electron transport compounds, such as 2-(4-biphenyl)-5-(4-*tert*-butylphenyl)-1,3,4-oxadiazole (PBD).<sup>3</sup> But the blended system may suffer from intrinsic phase separation. To address this issue, single polymers containing both hole- and electron-transporting moieties have been prepared. For example, polyfluorenes with either electron-withdrawing (such as oxadiazole, diphenylquinoline

etc.) or electron-donating groups (such as triphenylamine, carbazole etc.) integrated on the 9-position of fluorene have been reported as bipolar polymer host.<sup>4</sup>

Carbazole derivatives have played a very important role in organic/polymeric optoelectronic materials, and they can be used as host materials for both small molecule OLEDs (such as 4, 4'-*N,N'*-dicarbazole-biphenyl, CBP) and PLEDs (such as poly(vinylcarbazole), PVK) because of their high triplet energy and good hole-transporting ability.<sup>5</sup> But PVK has a HOMO level at about -5.9 eV and, consequently, a large barrier (about 1 eV) for hole injection from PEDOT:PSS. Furthermore, PVK is a unipolar conductor that transport

- (1) (a) Chen, F. C.; Yang, Y.; Thompson, M. E.; Kido, J. *Appl. Phys. Lett.* **2002**, *80*, 2038. (b) Gong, X.; Ostrowski, J. C.; Robinson, M. R.; Moses, D.; Bazan, G. C.; Heeger, A. J. *Adv. Mater.* **2002**, *14*, 581. (c) Gong, X.; Ostrowski, J. C.; Bazan, G. C.; Moses, D.; Heeger, A. J. *Appl. Phys. Lett.* **2003**, *81*, 3711. (d) Tokito, S.; Iijima, T.; Suzuri, Y.; Kita, H.; Tsuzuki, T.; Sato, F. *Appl. Phys. Lett.* **2003**, *83*, 569. (e) Holmes, R. J.; D'Andrade, B. W.; Forrest, S. R.; Ren, X.; Li, J.; Thompson, M. E. *Appl. Phys. Lett.* **2003**, *83*, 3818. (f) Zhang, K.; Chen, Z.; Yang, C.; Zhang, X.; Tao, Y.; Duan, L.; Chen, L.; Zhu, L.; Qin, J.; Cao, Y. *J. Mater. Chem.* **2007**, *17*, 3451.
- (2) (a) Sudhakar, M.; Djurovich, P. I.; Hogen-Esch, T. E.; Thompson, M. E. *J. Am. Chem. Soc.* **2003**, *125*, 7796. (b) Chen, F. C.; He, G.; Yang, Y. *Appl. Phys. Lett.* **2003**, *82*, 1006. (c) Adachi, C.; Kwong, R. C.; Djurovich, P.; Adamovich, V.; Baldo, M. A.; Thompson, M. E.; Forrest, S. R. *Appl. Phys. Lett.* **2001**, *79*, 2082. (d) Holmes, R. J.; Forrest, S. R.; Tung, Y. J.; Kwong, R. C.; Brown, J. J.; Garon, S.; Thompson, M. E. *Appl. Phys. Lett.* **2003**, *82*, 2422.

\* Corresponding author. E-mail: clyang@whu.edu.cn.

<sup>†</sup> Wuhan University.

<sup>‡</sup> Chinese Academy of Sciences.

holes only.<sup>6</sup> Recently, Brunner and co-workers reported that oligomers and polymers with carbazoles coupled via their 3/6 positions exhibit reversible oxidative behavior, and their HOMO levels can be tailored to match the Fermi levels of commonly used hole-injection layers PEDOT:PSS.<sup>7</sup> Moreover, the carbazoles maintain a sufficiently high triplet energy level due to the limited electronic conjugation of biphenyl upon oligomerization or polymerization. Chen et al. reported CBP-based polymer P(Bu-CBP) with high triplet energy of 2.53 eV, in which the additional carbazole group attached on the side chain can act as an inductive acceptor, leading to substantial lowering of the HOMO and LUMO levels with respect to poly(9-alkyl-carbazole-3,6-diyl)s, and they believe that the side group modification via the 9-position of carbazole allows a tuning of HOMO and LUMO levels to provide more balance in electron and hole fluxes.<sup>8</sup> However, there is a drawback of low fluorescence quantum efficiencies for poly(3, 6-cabazole) derivatives (about 5–15%).<sup>9</sup> Recently, Leclerc et al. developed well-defined and conjugated poly(2, 7-cabazole) derivatives with significantly improved PL quantum efficiencies.<sup>10</sup> Iraqi et al. investigated the properties of 2,7-linked *N*-functionalized carbazole polymers, and found that introducing electron-releasing 4-dialkylamino-phenyl substituents at the 9-position on carbazole repeat units results in higher HOMO level (−5.0 eV) than those poly(*N*-alkylcarbazole-2,7-diyl)s (−5.2 to −5.0 eV) and poly(*N*-arylcarbazole-2,7-diyl)s (−5.8 eV).<sup>11</sup>

In this work, with an aim to improve the electron-transporting ability of carbazole polymers, we prepared three copolymers containing carbazole main chain with oxadiazole moieties substituted at the 9-position of carbazole units, which serve as an independent electron-transporting group. We expect that the strong electron-withdrawing oxadiazole at 9-position of carbazole units could lower the HOMO/LUMO levels of the carbazole polymers to match the energy level of commonly used electrodes or neighboring layers, and the incorporation of the oxadiazole unit as bulky side group could improve the morphology stability and photoluminescence quantum efficiencies of polycarbazole. We also anticipate that the different coupling positions of carbazole units via 3,6-, 3,6-*alt*-2,7- or 2,7-linkage could tune the triplet energy of polycarbazoles.

## Experimental Section

**General Information.** <sup>1</sup>H NMR and <sup>13</sup>C NMR spectra were measured on Varian Unity 300 MHz spectrometer using CDCl<sub>3</sub> as solvent. Elemental analyses of carbon, hydrogen, and nitrogen were performed on a Carlorerba-1106 microanalyzer. The molecular weights of the polymers were determined by Agilent 1100 GPC in THF. The number-average and weight-average molecular weights were estimated by using a calibration curve of polystyrene standards. Differential scanning calorimetry (DSC) was performed on a NETZSCH DSC 200 PC unit at a heating rate of 10 °C min<sup>−1</sup> from 30 to 300 °C under argon. Thermogravimetric analysis (TGA) was undertaken with a NETZSCH STA 449C instrument. The thermal stability of the samples under a nitrogen atmosphere was determined by measuring their weight loss while heating at a rate of 20 °C min<sup>−1</sup> from 25 to 600 °C. UV–vis absorption spectra were recorded on Shimadzu UV-2550 spectrophotometer. PL spectra were recorded on Hitachi F-4500 fluorescence spectrophotometer. The PL quantum yields were measured from dilute toluene solution of copolymers **P1–3** (ca. 1 × 10<sup>−5</sup> mol/L) by an absolute method using the Edinburgh Instruments integrating sphere excited with Xe lamp. Cyclic voltammetry (CV) was carried out on a CHI voltammetric analyzer at room temperature in nitrogen-purged anhydrous acetonitrile with tetrabutylammonium hexafluorophosphate (TBAPF<sub>6</sub>) as the supporting electrolyte at scanning rate of 200 mV/s. Platinum disk and Ag/Ag<sup>+</sup> were used as working electrode and referenced electrode, respectively. Ferrocene was used for potential calibration. The onset potential was determined from the intersection of two tangents drawn at the rising and background current of the cyclic voltammogram.

All reagents commercial available were used as received unless otherwise stated. The solvents (THF, toluene) were purified by routine procedure and distilled under dry argon before using. All reactions were carried out using Schlenk techniques in an argon atmosphere. **1**,<sup>12</sup> **2**,<sup>13</sup> **3**,<sup>14</sup> **M3**, and **M4**<sup>15</sup> were prepared according to the published procedure. The synthesis of **M1** and **M2** are described in the Supporting Information.

**Preparation of the Polymers. P1:** A mixture of monomer **M1** (0.3 g, 0.5 mmol), **M3** (0.2 g, 0.5 mmol), Pd(PPh<sub>3</sub>)<sub>4</sub> (15 mg, 3% mmol), and K<sub>3</sub>PO<sub>4</sub>·4H<sub>2</sub>O (1.33 g, 5 mmol) in 5 mL of toluene

- (3) (a) Cao, Y.; Parker, I. D.; Yu, G.; Zhang, C.; Heeger, A. J. *Nature* **1999**, *374*, 414. (b) Jiang, C.; Yang, W.; Peng, J.; Xiao, S.; Cao, Y. *Adv. Mater.* **2004**, *16*, 537. (c) Tokito, S.; Suzuki, M.; Sato, F.; Kamachi, M.; Shirane, K. *Org. Electron.* **2003**, *4*, 105.
- (4) (a) Su, H. J.; Wu, F. I.; Shu, C. F.; Tung, Y. L.; Chi, Y.; Lee, G. H. *J. Polym. Sci., Part A: Polym. Chem.* **2005**, *43*, 859. (b) Liu, Z.; Zhang, Y.; Hu, Y.; Su, G.; Ma, D.; Wang, L.; Jing, X.; Wang, F. *J. Polym. Sci., Part A: Polym. Chem.* **2002**, *40*, 1122. (c) Shu, C. F.; Dodda, R.; Wu, F. I.; Liu, M. S.; Jen, A. K. Y. *Macromolecules* **2003**, *36*, 6698. (d) Wu, F. I.; Shih, P. I.; Shu, C. F.; Tung, Y. L.; Chi, Y. *Macromolecules* **2005**, *38*, 9028.
- (5) (a) Baldo, M. A.; Lamansky, S.; Burrows, P. E.; Thompson, M. E.; Forrest, S. R. *Appl. Phys. Lett.* **1999**, *75*, 4. (b) Lamansky, S.; Djurovich, P. I.; Abdel-Razzaq, F.; Garon, S.; Murphy, D. L.; Thompson, M. E. *J. Appl. Phys.* **2002**, *92*, 1570.
- (6) (a) Hong, H.; Sfez, R.; Yitzchaik, S.; Davidov, D. *Synth. Met.* **1999**, *102*, 1217. (b) Ohmori, Y.; Kajii, H.; Sawatani, T.; Ueta, H.; Yoshino, K. *Thin Solid Films* **2001**, *393*, 407. (c) Liang, C.; Li, W.; Hong, Z.; Liu, X.; Peng, J.; Liu, L.; Lu, Z.; Xie, M.; Liu, Z.; Yu, J.; Zhao, D. *Synth. Met.* **1997**, *91*, 151. (d) Lamansky, S.; Kwong, R. C.; Nugent, M.; Djurovich, P. I.; Thompson, M. E. *Org. Electron.* **2001**, *2*, 53.
- (7) (a) Dijken, A. V.; Bastiaansen, J. J. A. M.; Kiggen, N. M. M.; Langeveld, B. M. W.; Rothe, C.; Monkman, A. P.; Bach, I.; Stössel, P.; Brunner, K. *J. Am. Chem. Soc.* **2004**, *126*, 7718. (b) Brunner, K.; Dijken, A. V.; Bömer, H.; Bastiaansen, J. J. A. M.; Kiggen, N. M. M.; Langeveld, B. M. W. *J. Am. Chem. Soc.* **2004**, *126*, 6035.
- (8) Chen, Y. C.; Huang, G. S.; Hsiao, C. C.; Chen, S. A. *J. Am. Chem. Soc.* **2006**, *128*, 8549.
- (9) (a) Iraqi, A.; Wataru, I. *J. Polym. Sci., Part A: Polym. Chem.* **2004**, *42*, 6041. (b) Zhang, Z. B.; Fujiki, M.; Tang, H. Z.; Motonaga, M.; Torimitsu, K. *Macromolecules* **2002**, *35*, 1988.
- (10) (a) Zotti, G.; Schiavon, G.; Zecchin, S.; Morin, J. F.; Leclerc, M. *Macromolecules* **2002**, *35*, 2122. (b) Morin, J. F.; Beaupré, S.; Leclerc, M.; Lévesque, I.; D'iorio, M. *Appl. Phys. Lett.* **2002**, *80*, 341. (c) Morin, J. F.; Leclerc, M. *Macromolecules* **2002**, *35*, 8413.
- (11) (a) Iraqi, A.; Wataru, I. *Chem. Mater.* **2004**, *16*, 442. (b) Iraqi, A.; Pickup, D. F.; Yi, H. *Chem. Mater.* **2006**, *18*, 1007. (c) Iraqi, A.; Simmance, T. G.; Yi, H. N.; Stevenson, M.; Lidzey, D. G. *Chem. Mater.* **2006**, *18*, 5789. (d) Iraqi, A.; Pegington, R. C.; Simmance, T. G. *J. Polym. Sci., Part A: Polym. Chem.* **2006**, *44*, 3336. (e) Yi, H. N.; Iraqi, A.; Stevenson, M.; Elliott, C. J.; Lidzey, D. G. *Macromol. Rapid Commun.* **2007**, *28*, 1155.

- (12) Sharma, G. V. M.; Begum, A.; Rakesh; Krishna, P. R. *Synth. Commun.* **2004**, *34*, 2387.
- (13) Stephen, O.; Vial, J. C. *Synth. Met.* **1999**, *106*, 115.
- (14) Freeman, A. W.; Urvoy, M.; Criswell, M. E. *J. Org. Chem.* **2005**, *70*, 5014.
- (15) (a) Huang, J.; Niu, Y. H.; Yang, W.; Mo, Y.; Yuan, M.; Cao, Y. *Macromolecules* **2002**, *35*, 6080. (b) Pan, X.; Liu, S.; Chan, H. S. O.; Ng, S. C. *Macromolecules* **2005**, *38*, 7629.

and 2 mL of distilled water in a Schlenk tube was stirred at 100 °C for 72 h. The resulting polymers were purified by precipitation in methanol twice and washed with acetone in a Soxhlet apparatus for 72 h. **P1** was obtained as gray powder with a yield of 70%. <sup>1</sup>H NMR (300 MHz, CDCl<sub>3</sub>, δ): 8.50–8.38, 8.25–8.04, 7.85–7.57, 7.50–7.44, 7.07–6.99, 4.22, 3.95, 2.02, 1.74, 1.34, 0.93. <sup>13</sup>C NMR (75 MHz, CDCl<sub>3</sub>, δ): 163.74, 162.52, 161.29, 139.54, 138.48, 134.00, 131.58, 131.19, 127.67, 127.45, 127.31, 124.35, 123.74, 122.59, 119.37, 117.66, 115.03, 114.05, 109.01, 108.26, 69.83, 46.41, 38.36, 30.02, 29.51, 28.09, 27.82, 23.41, 22.87, 22.02, 13.04, 10.11, 9.91. Anal. Calcd for C<sub>54</sub>H<sub>56</sub>N<sub>4</sub>O<sub>2</sub>: C, 81.78; H, 7.12; N, 7.06. Found: C, 82.40; H, 6.65; N, 6.82.

**P2** was obtained as gray powder with a yield of 67% by the same procedure with **P1**. **M2** (0.3 g, 0.5 mmol), **M3** (0.2 g, 0.5 mmol), Pd(PPh<sub>3</sub>)<sub>4</sub> (15 mg, 3% mmol), and K<sub>3</sub>PO<sub>4</sub>·4H<sub>2</sub>O (1.33 g, 5 mmol). <sup>1</sup>H NMR (300 MHz, CDCl<sub>3</sub>, δ): 8.36, 8.19, 8.01, 7.75, 7.42, 6.96, 4.16, 3.84, 2.07, 1.67, 1.28, 0.87. <sup>13</sup>C NMR (75 MHz, CDCl<sub>3</sub>, δ): 163.75, 162.49, 161.21, 140.47, 139.79, 139.44, 131.90, 127.60, 126.50, 124.71, 122.44, 122.28, 121.86, 121.70, 121.24, 119.62, 118.23, 118.03, 117.80, 114.83, 113.96, 108.35, 107.10, 69.66, 46.46, 38.41, 38.21, 29.97, 29.39, 27.99, 27.86, 23.36, 22.73, 22.05, 21.98, 13.06, 10.06, 9.88. Anal. Calcd for C<sub>54</sub>H<sub>56</sub>N<sub>4</sub>O<sub>2</sub>: C, 81.78; H, 7.12; N, 7.06. Found: C, 80.84; H, 6.58; N, 6.74.

**P3** was obtained as gray powder with a yield of 55% by the same procedure with **P1**. **M2** (0.3 g, 0.5 mmol), **M4** (0.2 g, 0.5 mmol), Pd(PPh<sub>3</sub>)<sub>4</sub> (15 mg, 3% mmol), and K<sub>3</sub>PO<sub>4</sub>·4H<sub>2</sub>O (1.33 g, 5 mmol). <sup>1</sup>H NMR (300 MHz, CDCl<sub>3</sub>, δ): 8.47, 8.30, 8.14, 7.96, 7.85, 7.77, 7.69, 7.60, 7.09, 4.30, 3.97, 2.16, 1.79, 1.28, 0.98. <sup>13</sup>C NMR (75 MHz, CDCl<sub>3</sub>, δ): 164.89, 163.45, 162.35, 142.02, 141.53, 140.79, 139.57, 128.71, 127.54, 122.70, 121.86, 120.80, 119.05, 115.86, 115.08, 108.62, 107.88, 70.71, 39.27, 30.99, 30.44, 29.05, 28.82, 24.39, 23.78, 23.03, 14.11, 11.11, 10.09. Anal. Calcd for C<sub>54</sub>H<sub>56</sub>N<sub>4</sub>O<sub>2</sub>: C, 81.78; H, 7.12; N, 7.06. Found: C, 82.20; H, 6.72; N, 6.60.

**PLED Fabrication and Measurements.** The devices were fabricated according to the configurations of ITO/PEDOT:PSS/polymer:Ir(ppq)<sub>2</sub>(acac)(5 wt %)/BCP/AlQ/LiF/Al. Commercial indium tin oxide (ITO) coated glass with sheet resistance of 10 Ω/□ was used as the starting substrates. Before device fabrication, the ITO glass substrates were pre-cleaned carefully and treated with O<sub>2</sub> plasma for 2 min. A 50 nm thick poly(ethylenedioxythiophene):poly(styrenesulfonic acid) (PEDOT:PSS) film was then spin-coated from a water solution onto ITO glass substrates, and cured at 110 °C for 30 min. About 80 nm of the mixture of Ir(ppq)<sub>2</sub>(acac) and polymer host was spin-coated from a chloroform solution with a total concentration of 10 mg/mL. Then the sample was transferred to the deposition system for organic and metal deposition. Ten nanometer 2,9-dimethyl-4,7-diphenyl-1,10-phenanthroline (BCP) as a hole and exciton blocking layer, 40 nm of Alq<sub>3</sub> as the electron transporting layer, and a cathode composed of 1 nm of lithium fluoride and 120 nm of aluminum were sequentially deposited onto the substrate in the vacuum of 1 × 10<sup>-6</sup> Torr. The *I*–*V*–*B* of EL devices was measured with a Keithley 2400 Source meter and a Keithley 2000 Source multimeter equipped with a calibrated silicon photodiode. The EL spectra were measured by JY SPEX CCD3000 spectrometer. All the experiments and measurements were carried out at room temperature under ambient conditions.

## Results and Discussion

**Synthesis and Characterization.** The synthetic routes of the monomers and copolymers are depicted in Scheme 1. The carbazole-based monomers (**M1** and **M2**) with the oxadiazole moiety substituted at the 9-position of carbazole

was synthesized through an aromatic nucleophilic substitution reaction of arylamine and fluoroarenes activated by the electron-withdrawing oxadiazole, with good yields of more than 80%.<sup>16</sup> Copolymers were prepared via Suzuki coupling reactions between dibromomides (**M1** and **M2**) and diboronates (**M3** and **M4**). The resulting copolymers can be readily dissolved in common organic solvents, such as chloroform, toluene, and THF. The structures of these polymers were characterized by <sup>1</sup>H NMR, <sup>13</sup>C NMR and elemental analysis. Gel-permeation chromatography (GPC) analysis with polystyrene standards showed number-averaged molecular masses (*M<sub>n</sub>*) are in the range of 5279 and 7634 g/mol with good polydispersities index between 1.39 and 1.78 (Table 1).

**Thermal Analysis.** The thermal stabilities of the copolymers were investigated by thermal gravimetric analysis (TGA) under nitrogen (Figure 1 and Table 1). The decomposition patterns of the three polymers are similar, with 5% weight loss temperatures ranging from 412 to 435 °C, which indicated their good thermal stability. Thermal induced phase transition behaviors of the copolymers were studied by differential scanning calorimetry (DSC) in nitrogen atmosphere, and the results revealed that **P1**, **P2**, and **P3** are amorphous solids with high glass transition temperatures (*T<sub>g</sub>*) at 211, 194, and 208 °C, respectively. The values are much higher than the analogous poly(9-alkyl-9*H*-carbazole-3,6-diyl)s (142 °C)<sup>9b</sup> and poly(9-alkyl-9*H*-carbazole-2,7-diyl)s (68 °C),<sup>10c</sup> implicating that the introduction of oxadiazole side chain could greatly improve the morphological stability of the polymers.

**Photophysical Properties.** The electronic and photoluminescent spectra of the polymers were investigated both in dilute toluene solution and in solid state film on quartz substrate (Figure 2). The photophysical data are summarized in Table 1. **P1** exhibits an absorption peak at 303 nm and a shoulder at 355 nm in toluene solution, and the peak at 303 nm is close to that in poly(9-alkyl-carbazole-3,6-diyl)s (308 nm).<sup>9</sup> **P2** and **P3** show broad absorption bands centered at 349 and 370 nm, respectively. The band gaps (*E<sub>g</sub>*) of **P1**, **P2**, and **P3** as determined from the onset wavelength of absorption bands are 3.01, 2.98, and 2.87 eV, respectively. The absorption red-shift, together with the decreasing band gap from **P1** to **P3** imply that the extent of  $\pi$  conjugation along the polymer backbone is enlarged from **P1** to **P3**. In fact, the conjugation segments in **P1** and **P2** can be described as biphenyl and triphenyl, respectively, whereas the 2,7-linked **P3** is conjugated along the whole backbone.<sup>17</sup>

The polymers show deep blue emission with PL peaks in the range of 400 and 431 nm in toluene solution. The PL peaks in the solid state film are red-shifted by 20–40 nm with respect to their polymer solution. The Stokes shift of **P1** (76 nm) is remarkably larger than those of **P2** (51 nm) and **P3** (40 nm), which implies larger structural differences between the ground and excited states in **P1**. The fluorescence quantum yields of the polymers were measured in toluene solution at the concentration of 1 ×

(16) (a) Gorvin, J. H. *J. Chem. Soc., Perkin Trans. I* **1988**, 1331. (b) Zhang, K.; Zou, Y.; Xu, X.; Gong, S.; Yang, C.; Qin, J. *Macromol. Rapid Commun.* (DOI: 10.1002/marc200800521).



Scheme 1. Synthesis of the Monomers (M1–2) and Copolymers P1–3

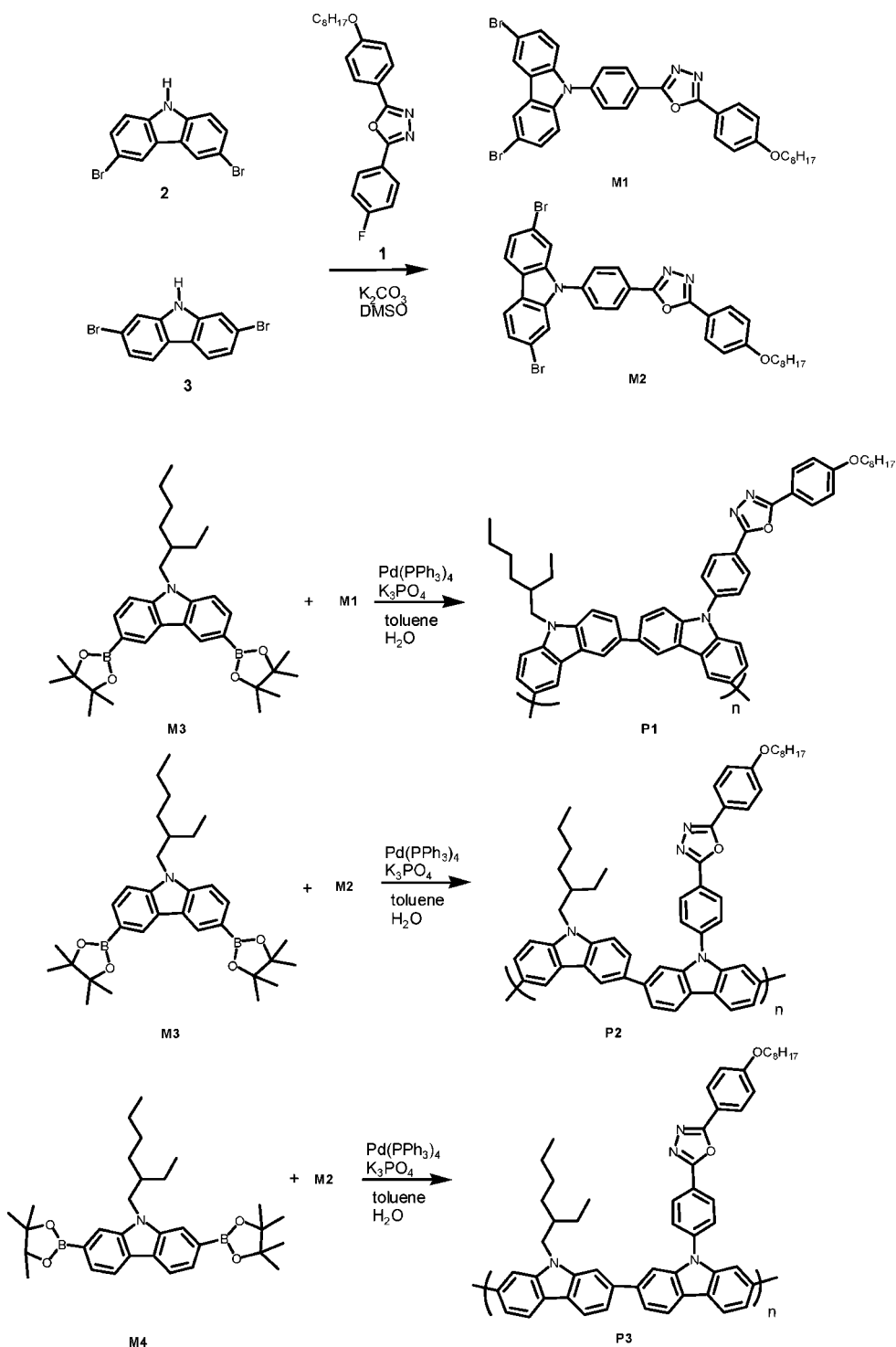


Table 1. Structural and Thermal Data of the Polymers

	Mn <sup>a</sup>	PDI	T <sub>d</sub> (°C)	T <sub>g</sub> (°C)
<b>P1</b>	5279	1.39	421	211
<b>P2</b>	5219	1.36	435	194
<b>P3</b>	7634	1.78	412	208

<sup>a</sup> Molecular weights were determined by GPC using polystyrene standards.

$10^{-5}$  M by absolute method using the Edinburgh Instruments integrating sphere excited at their maximum absorption wavelength. PL quantum yields of **P1** and **P2** are significantly enhanced by 47.8 and 62.1%, respectively,

compared to their analogous polymers, such as poly(*N*-alkyl-carbazole-3,6-diyl)s (5–15%)<sup>9</sup> and poly(fluorene-*alt*-carbazole) (PFCz) (25%).<sup>18</sup> **P3** also shows a higher PL quantum yield of 87.6% than its analogous poly(9-alkyl-carbazole-2,7-diyl)s (ca. 70%).<sup>10</sup> The results suggest that the bulky oxadiazole on the 9-position of carbazole could improve the PL quantum efficiencies of polycarbazoles.

The triplet emission spectra of the copolymers were recorded at low temperature (77 K) upon excitation with 350 nm (Figure 3), and the highest-energy vibronic subband ( $T_1^{\nu=0} \rightarrow S_1^{\nu=0}$ ) was taken as measure for the triplet energy

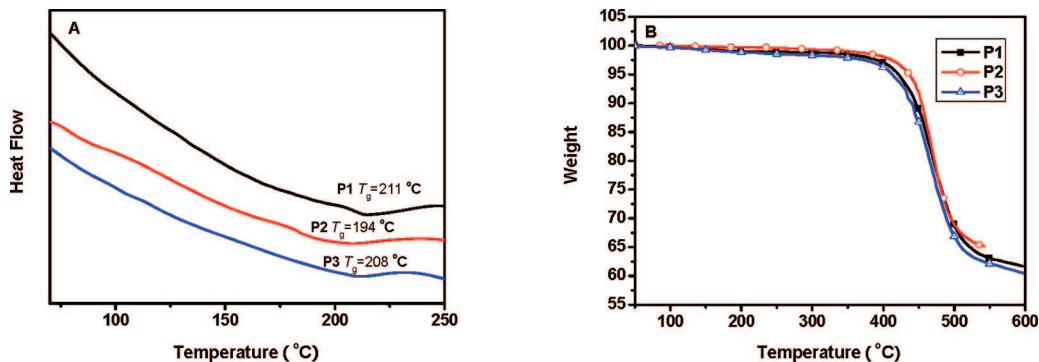


Figure 1. (A) DSC and (B) TGA thermograms of P1–3.

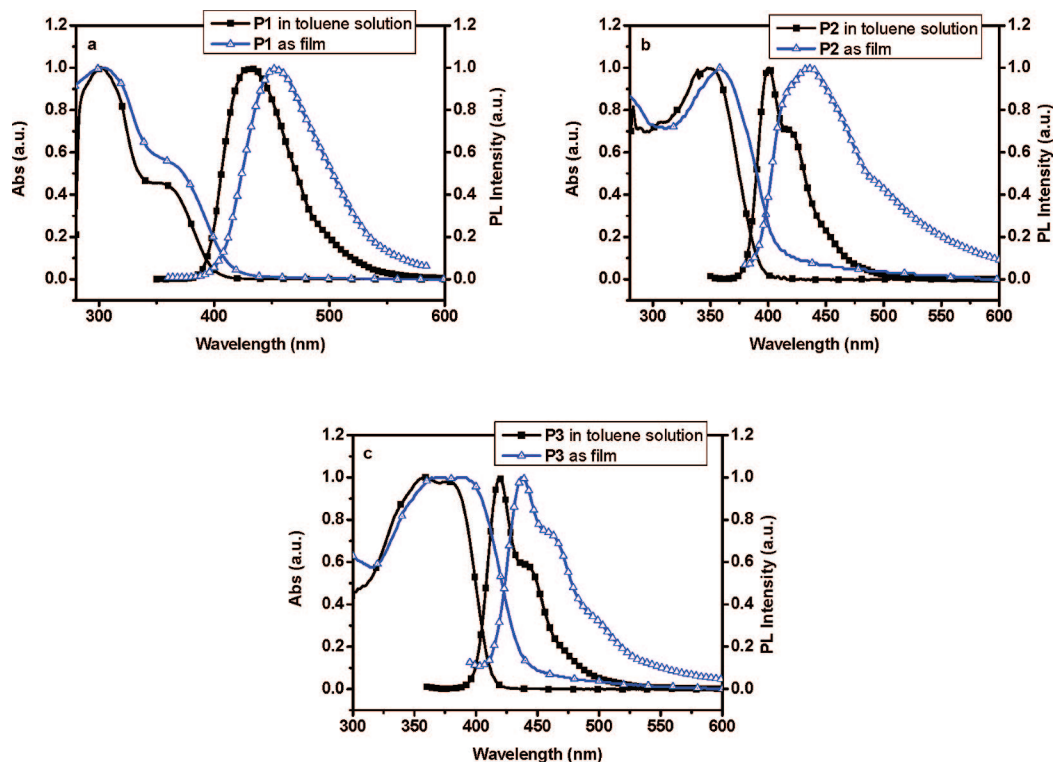


Figure 2. UV-vis absorption and PL spectra of (a) P1, (b) P2, and (c) P3 in dilute toluene solution and in solid-state film.

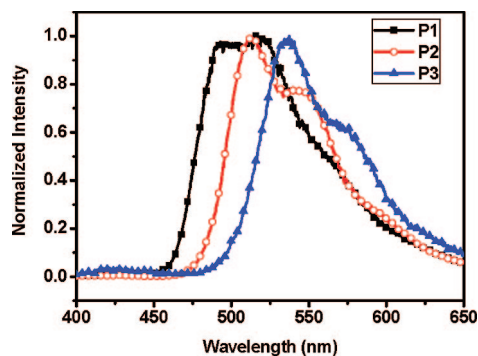


Figure 3. Triplet emission spectra of P1–3 in solid state film at 77 K upon excitation with 350 nm.

( $E_T$ ) of the polymers.<sup>7a</sup>  $E_T$  of P1 (2.52 eV, 492 nm) is close to that of typical poly(3,6-carbazole) (ca. 2.6 eV).<sup>8</sup> P2 possesses a slightly larger  $\pi$ -electron delocalization over the *p*-terphenyl than *p*-biphenyl conjugation length in P1, and thus the  $E_T$  of P2 decreases to 2.42 eV (512 nm).  $E_T$  of P3 further drops to 2.32 eV (534 nm) because of its poly(*p*-

phenylene)-like molecular structure. This demonstrates that the triplet energy of polycarbazoles can be tuned by different coupling positions of carbazole units.

**Electrochemical Properties.** To study the electrochemical properties of the polymers, cyclic voltammetry (CV) measurements on drop-cast polymer films were conducted in acetonitrile with tetrabutylammonium hexafluorophosphate (TBAPF<sub>6</sub>) as the supporting electrolyte. The obtained CV curves were referenced to an Ag/Ag<sup>+</sup> electrode (0.1 M AgNO<sub>3</sub> in acetonitrile), which was calibrated using the ferrocene/ferrocenium redox couple (0.1 V vs Ag/Ag<sup>+</sup>) as an internal standard. The HOMO levels of copolymers P1–3 are determined from onset potential of first oxidation peak during anodic sweep in the cyclic voltammetry measurements with regard to the energy levels of ferrocene reference (4.8 eV below the vacuum level).<sup>19</sup> The reduction waves of copolymers P1–3 were either irreversible or hardly to be

(17) (a) Rothe, C.; Brunner, K.; Bach, I.; Heun, S.; Monkman, A. P. *J. Chem. Phys.* **2005**, *122*, 84706–1. (b) Higuchi, J.; Hayashi, K.; Yagi, M.; Kondo, H. *J. Phys. Chem. A* **2002**, *106*, 8609.

**Table 2. Photophysical Data of the Polymers**

	$\lambda_{\text{abs}}$ (nm) solution <sup>a</sup> /film <sup>b</sup>	$\lambda_{\text{PL}}$ (nm) solution <sup>a</sup> /film <sup>b</sup>	fwhm <sup>a</sup> (nm)	Stokes shift <sup>a</sup> (nm)	$Q_{\text{PL}}$ <sup>a</sup> (%)	$E_{\text{T}}$ <sup>b</sup> (eV)
<b>P1</b>	303(355)/304(362)	431/451	78	76	47.8	2.52
<b>P2</b>	349/357	400(418)/435(419)	82	51	62.1	2.42
<b>P3</b>	358(379)/370(390)	419(440)/437(460)	55	40	87.6	2.32

<sup>a</sup> Measured in toluene solution. <sup>b</sup> Measured in solid-state film.

**Table 3. Electrochemical Data of the Copolymers**

	$E_{\text{oxd}}^{\text{onset}}$ (V) <sup>a</sup>	HOMO (eV) <sup>b</sup>	$E_{\text{g}}$ (eV) <sup>c</sup>	LUMO (eV) <sup>d</sup>
<b>P1</b>	0.56	-5.26	3.01	-2.25
<b>P2</b>	0.68	-5.38	2.98	-2.40
<b>P3</b>	0.90	-5.60	2.87	-2.73

<sup>a</sup> Onset oxidation potential vs Ag/AgNO<sub>3</sub>. <sup>b</sup> Estimated from the onset oxidation potential. <sup>c</sup> Estimated from the onset of absorption edge. <sup>d</sup> Deduced from HOMO and  $E_{\text{g}}$ .

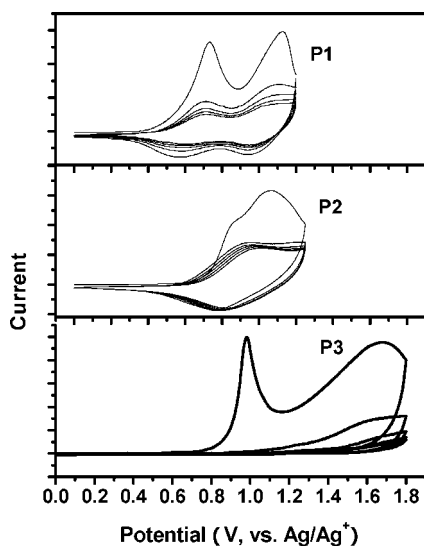


**Figure 4.** CV curves of **P1** (up), **P2** (middle), and **P3** (bottom) as films upon repeated 5 cycles at a scan rate of 200 mV/s.

observed, and thus the LUMO levels were deduced from HOMO levels and energy gaps determined by the onset of absorption spectra. Electrochemical data of **P1–3** are listed in Table 3.

As shown in Figure 4, **P1** exhibits two reversible oxidation peaks at 0.73 and 1.12 V with two corresponding counter-cathodic peaks at 0.58 and 0.95 V. The two reversible redox waves could be assigned to the two kinds of 3,6-linked carbazole units on the backbone of **P1**. The HOMO level of **P1** (-5.26 eV) is close to that of the *N*-aryl poly(3,6-cabazole), such as CBP-based polymer P(<sup>t</sup>Bu-CBP) (-5.3 eV), and significantly lower than that of *N*-alkyl poly(3,6-cabazole), such as poly(9-*n*-octyl-carbazole-3,6-diyl)s (-5.0 eV).<sup>8</sup> This means that the hole-injection barrier for **P1** at the interfaces with PEDOT:PSS is significantly decreased relative to those of the common polymer hosts PFOs/PEDOT:PSS (0.6–0.8 eV) and PVKs/PEDOT:PSS (~1 eV). Simultaneously, the LUMO level of **P1** (-2.25 eV) is substantially decreased in comparison with P(<sup>t</sup>Bu-CBP) (-2.04 eV) and poly(9-*n*-octyl-carbazole-3,6-diyl)s (-1.8

eV).<sup>8</sup> This represents a small barrier for electron injection from commonly used cathode such as barium (work function of 2.2 eV).

Upon repeated scan (between 0 and 1.8 V vs Ag/Ag<sup>+</sup>), **P3** shows two irreversible oxidation peaks at 0.95 and 1.59 V. The oxidation peaks decreased significantly on the second cycle and could hardly be seen during the third cycle, which indicates its unstable electrochemical property. Such instability is attributed to the formation of new species as a results of cross-linkage through the active 3,6-position during the CV measurement.<sup>10a</sup> The HOMO and LUMO levels of **P3** (-5.6/-2.73 eV) are substantially lowered with respect to those of the *N*-alkyl poly(2,7-carbazole), poly(9-alkyl-9H-carbazole-2,7-diyl)s (-5.4 eV/-2.5 eV).<sup>11</sup> **P2** with carbazole derivatives coupled alternatively via 3,6- and 2,7-positions has a similar energy gap of 2.98 eV to **P1**. Repeating anodic scan between 0 and 1.3 V, **P2** undergoes one reversible oxidation wave peaked at 0.9 V with corresponding reduction wave peaked at 0.78 V. The HOMO and LUMO levels of **P2** (-5.38/-2.40 eV) are between **P1** and **P3**. The LUMO level is close to those reported for the electron-transporting material, such as OXD-substituted PF (-2.47 eV) and 2-(4-biphenyl)-5-(4-*tert*-butylphenyl)-1,3,4-oxadiazole (PBD) (-2.4 eV).<sup>20,3a</sup>

**Electroluminescence.** The polymers have higher triplet energy (**P1**, 2.52 eV; **P2**, 2.42 eV; **P3**, 2.32 eV) than that of red phosphorescent emitter: bis(2,4-diphenylquinolino-*N,C*<sup>2'</sup>)iridium(acetylacetonate) (Ir(ppq)<sub>2</sub>(acac),  $E_{\text{T}} = 2.00$  eV);<sup>21</sup> therefore, they are all potential hosts for the guest. Polymer light-emitting diodes with the device configurations of ITO/PEDOT:PSS (50 nm)/polymer:Ir(ppq)<sub>2</sub>(acac) (5 wt %) (80 nm)/BCP (10 nm)/AlQ (40 nm)/LiF (1 nm)/Al (120 nm) were fabricated by using **P1–3** as host materials doped with Ir(ppq)<sub>2</sub>(acac) as triplet emitter, where the polyethylene dioxythiophene:polystyrene sulfonate (PEDT:PSS) was used as the hole-injection layer, and 2,9-dimethyl-4,7-diphenyl-1,10-phenanthroline (BCP) was used as the hole-blocking layer and inserted between the emitting layer and the electron-transport tris-(8-hydroxyquinoline)aluminum to provide exciton and carrier confinement.<sup>22</sup> The proposed energy-level diagram for device components and the molecular structures of the compounds used in the device are shown in Figure 5.

As shown in Figure 6, these devices exhibit saturated red emission with the peak at 620 nm originating from Ir(ppq)<sub>2</sub>(acac). Furthermore, no emission from host polymers is observed, indicating complete energy transfer from polymer host to the iridium complex at the doping level at 5 wt %.

Figure 7 shows the current density–voltage–luminance characteristics of the devices. The maximum luminance of 1111 cd/m<sup>2</sup> at 538 mA/cm<sup>2</sup>, 1060 cd/m<sup>2</sup> at 605 mA/cm<sup>2</sup>, and 382 cd/m<sup>2</sup> at 185 mA/cm<sup>2</sup> are obtained for devices made from **P1**, **P2**, and **P3**, respectively. The devices are lighted

(18) Zhang, K.; Chen, Z.; Yang, C.; Gong, S.; Qin, J.; Cao, Y. *Macromol. Rapid Commun.* **2006**, *27*, 1926.  
(19) Pommerehne, J.; Vestweber, H.; Guss, W.; Mahrt, R. F.; Baessler, H.; Porsch, M.; Daub, J. *Adv. Mater.* **1995**, *7*, 551.

(20) Wu, F. I.; Reddy, D. S.; Shu, C. F.; Liu, M. S.; Jen, A. K. Y. *Chem. Mater.* **2003**, *15*, 269.  
(21) Wu, F. I.; Su, H. J.; Shu, C. F.; Luo, L.; Diau, W. G.; Cheng, C. H.; Duan, J. P.; Lee, G. H. *J. Mater. Chem.* **2005**, *15*, 1035.  
(22) Ding, J.; Gao, J.; Fu, Q.; Cheng, Y.; Ma, D.; Wang, L. *Synth. Met.* **2005**, *155*, 539.

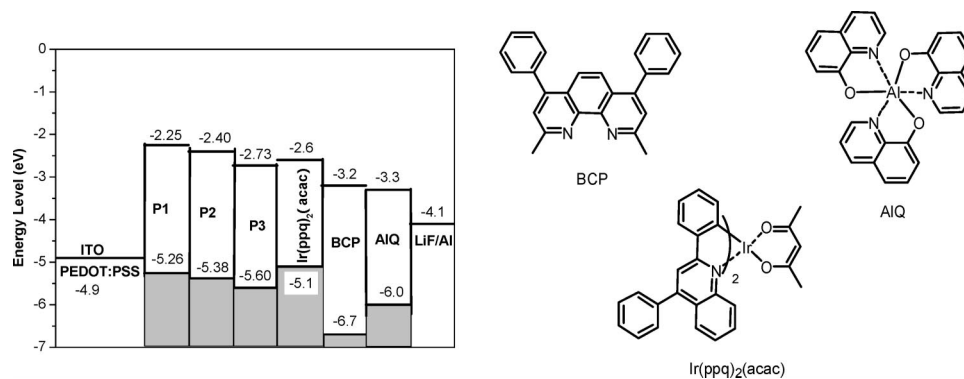


Figure 5. Proposed energy-level diagram for device components and the compounds used in the device.

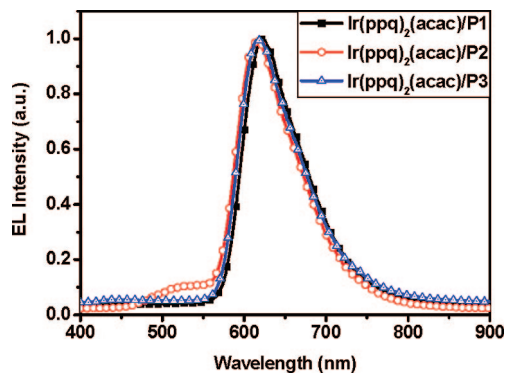


Figure 6. Electroluminescence spectra of **P1**–**3** doped with  $\text{Ir}(\text{ppq})_2(\text{acac})$  (5 wt %).

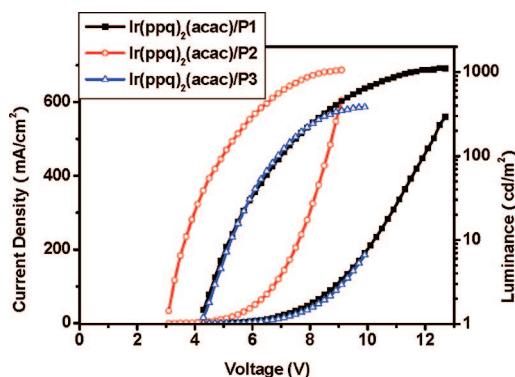


Figure 7. Current density and luminance vs voltage for PLEDs.

(with luminance at  $1 \text{ cd/m}^2$ ) at low turn-on voltage of 3.1–4.3 V, which are comparable with devices from  $\text{Ir}(\text{piq})_2(\text{acac})$  (bis(1-phenyl-isoquinolino- $N, C^2$ )iridium(acetylacetonate)) doped with P(*t*Bu-CBP) (3.0 V), and  $\text{Ir}(\text{FPQ})_2(\text{acac})$  (bis(2-(9,9-di-*n*-octylfluorene-2-yl)-4-phenylquinoline)iridium(acetylacetonate)) doped in PF-TPA-OXD (4.2 V).<sup>8,23</sup> This means effective carrier injection into the emitting layer from adjacent hole-injecting layer and hole-blocking layer.

Figure 8 shows current efficiency as a function of current density for the devices. The maximum current efficiencies for the **P1**–**3** based devices are 0.59, 1.33, and 1.67 cd/A, respectively, which are comparable to the performance from the device from  $\text{Ir}(\text{piq})_2(\text{acac})$  doped in poly(9-alkyl-9H-

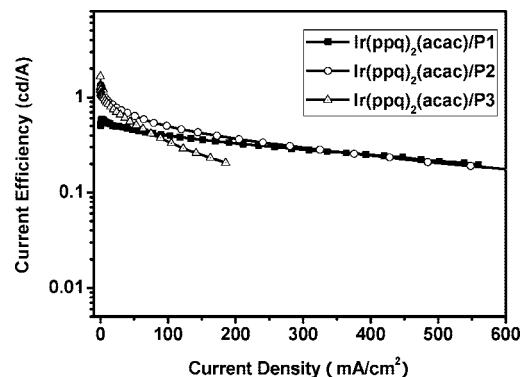


Figure 8. External quantum efficiencies vs current density for PLEDs.

carbazole)-3,6-diyls ( $1.2 \text{ cd/A}$ ).<sup>8</sup> The devices from **P2** and **P3** show higher efficiency than that from **P1**. Considering the triplet energy level of the three host materials are higher than the phosphorescent emitter, the improvement could be partially due to the higher PL quantum efficiencies of **P2** and **P3**, which may lead to a more efficient Förster energy transfer from the host to the guest.

## Conclusions

In conclusion, three new polycarbazoles with oxadiazole pendant were designed and synthesized toward bipolar polymer host. The thermal, electrical and optical properties of the polycarbazoles depend on the coupling positions of carbazole units and the substituents at the 9-position of carbazole. The substitution of diaryl-1,3,4-oxadiazole at the 9-position of carbazole leads to significantly enhanced thermal stability and fluorescence quantum efficiencies compared to analogous 9-alkyl substituted polycarbazoles. **P1** by connecting carbazole units via their 3 (6) positions shifts the HOMO/LUMO levels to higher energy compared to **P3** via 2 (7) positions, whereas replacing alkyl groups at the 9-position of carbazole on polycarbazoles with electron-withdrawing diaryl-1,3,4-oxadiazole group shifts the HOMO/LUMO levels to lower energy. Without changing the composition of the polycarbazoles, the triplet energy can be tuned by changing the way in which the different monomers are coupled together. **P1** has a higher triplet energy than **P3** because of the limited electronic conjugation of biphenyl in **P1**. These design rules can be applied to tune the energy levels in a wide range, and thus make hosts for PLEDs that not only have proper triplet energies but also matchable

(23) Wu, F. I.; Shih, P. I.; Tseng, Y. H.; Chen, G. Y.; Chien, C. H.; Shu, C. F.; Tung, Y. L.; Chi, Y.; Jen, A. K. Y. *J. Phys. Chem. B* **2005**, *109*, 14000.

energy levels for charge injection from neighboring layers. Polymer light-emitting diodes employing the **P1–3** as hosts and bis(2,4-diphenylquinolino-*N,C*<sup>2'</sup>)iridium(acetylacetonate) (Ir(ppq)<sub>2</sub>(acac)) as guest show low turn-on voltage from 3.1 to 4.3 V, implying effective and balanced carrier injection into the emitting layer from adjacent layers. We believe the device performance can be further improved by choosing a suitable electro-transport and hole blocking layer with matching LUMO level like TPBI (6.4 eV for HOMO, 2.7 eV for LUMO) to lower the electron injection barrier.

**Acknowledgment.** We thank the National Natural Science Foundation of China (Projects 50773057 and 20474047) and the Program for New Century Excellent Talents in University, the Ministry of Education of China (NCET-04-0682) for financial support.

**Supporting Information Available:** Preparation of **M1** and **M2**; <sup>1</sup>H NMR of **P1–3** (PDF). This material is available free of charge via the Internet at <http://pubs.acs.org>.

CM802240Q